Journal of Mathematical Modeling and Fractional Calculus

Website: https://acspublisher.com/journals/index.php/jmmfc

Received:03-10-24, **Revised:** 16-11-24,
Accepted: 02-12-24, **Publication:** 31-12-24
https://doi.org/10.48165/jmmfc.2024.1205**,**1(2),72-98

Dynamical transmission of Varicella Virus in Jordan with SVIR Model through analysis and numerical simulations

Manal Ghannam[a,b]

[a] Faculty of Art and Sciences, Department of Mathematics, Near East University, Northren Cyprus, Turkey
[b] Mathematical research center, Near East University, Northren Cyprus, Turkey
Corresponding author manal.ghannam@neu.edu.tr,

Abstract:

Chickenpox, another name for varicella virus, is a highly contagious illness. In this work, we use mathematical modelling and simulation to examine the dynamics of transmission and propose an SVIR model for the varicella virus in Jordan. The dynamics of the population in various classes are examined using a suggested model, which offers a more thorough comprehension of the course of the epidemic and the efficacy of control efforts. Lipschitz condition and fixed-point theory were also used to establish the solution's existence and uniqueness. Additionally, using figures and mathematics, it investigates the effects of different factors on the reproductive number R_0 and sensitivity analysis of the suggested model. The Routh-Hurwitz stability criterion is used to determine local stability at equilibrium sites that are both disease-free and endemic. Lyapunov functions with the first derivative test used to establish the global stability of model equilibria analysis for both $R_0>1$ and $R_0<1$.

the suggested model is numerically simulated using Matlab software to ascertain how parameters affect the scenarios. The findings of this study confirm the theoretical and biological phenomena of the model and aid in elucidating the mechanisms of varicella virus transmission and directing public safety policy decisions. In the conclusion, Since the varicella virus puts a lot of demand on the country's healthcare system, the Jordanian Ministry of Health should launch vaccination campaigns in order to eliminate the disease because a universal varicella vaccination is necessary. Long-lasting protection from varicella immunization lowers the risk of epidemics and promotes community health, and lowering the overall burden of varicella virus infection frees up funds for other health concerns.

Keywords: Varicella virus, Routh-Hurwitz stability, Sensitivity analysis, Basic reproduction Number.

1. Intorduction

Varicella virus is one of a very dangerous infectious disease. The earliest symptoms for this disease typically appear two to three weeks after infection. Fever, fatigue, and a lack of appetite were the first symptoms, which were followed by a broad rash. The rash starts off as red, itchy areas and soon turns into blisters, which are more common on the head, arms, legs, and face. Before the blisters dry out and heal, they stay there for three to four days. Healthy children and adults often recover in ten days [1-2]. Although paracetamol can be used to lower the temperature, most people don't require medical assistance. Rest and hydration are recommended. Infection risk can be decreased by keeping nails short and applying anti-itch soaps and creams [3-4].

A vaccination was developed and tested experimentally in the 1970s and 1980s. These days, these vaccinations might be either the varicella vaccine alone or the Measles, Mumps, and Rubella (MMR) vaccine, which combines the measles, mumps, and rubella vaccines [5-6].

Although this virus is believed to be a mild childhood illness, it can have major effects on certain groups of people, such as adults and those with weakened immune systems [7-8]. The development of mathematical methods for analysing communicable illnesses has led to an ideological split between public health professionals looking for workable disease management techniques and mathematicians seeking a thorough understanding. [9-15].

A vaccination campaign's effectiveness can be evaluated by mathematical modelling due to the complexity of the virus transmission dynamics and the interaction between direct and indirect vaccine effects. A number of mathematical models looked at the impacts of varicella vaccination in an effort to add to the conversation. [16-20].

The main aim of this work is to use the epidemiological data currently available to develop and assess a Suscibtible, Vaccinated, Infected, and Recovered (SVIR) model that is uniquely tailored to the dynamics of varicella virus spread in Jordan. By examining the key parameters of the SVIR model, which aids the government in developing new policies and strategies for future occurrences of circumstances like the one that is currently occurring. It is crucial to research the dynamics of varicella virus transmission in Jordan, especially in light of the current circumstances, in order to act quickly before the number

of infections skyrockets. As indicated in table (1.1), 82856 cases of chickenpox were reported in Jordan between 2008 and 2021 [21-22].

Table 1.1 History of the varicella virus in Jordan, 2008–2021 [23]

Year	2008	2009	2010	2011	2013	2014	2015	2017	2018	2019	2020	2021
Varecella Virus Cases × 1000	11.36	6.91	9.36	6.18	6.71	7.89	4.72	6.88	6.21	3.51	1.00	1.63

The immigration of Syrian refugees was responsible for 19.24% of the increase in total cases in 2014, while COVID-19 and the quarantine during the pandemic—particularly the closure of clinics and schools—were responsible for the lowest number of cases (2.44%) in 2020 [24]. Individuals who have contracted the varicella virus can easily spread the infection to people who have never had the virus or have not been vaccinated against it. Up to 90% of a person's close non-immune contacts will also contract it if they do[25]. It is predicted that the likelihood of the varicella virus spreading among susceptible people is approximately 0.09 [26].

2. Model assumption and formulation

Recent years have seen a steady rise in the occurrence of chickenpox in Jordan, highlighting the need for a deeper comprehension of its epidemiology. The SVIR model theoretical framework of the varicella virus in Jordan offers a conceptual foundation for understanding the dynamics of varicella virus transmission as well as the factors and characteristics influencing its transmission. There are four compartments in the SVIR model.

Those who are susceptible could contract the virus. Those who received the vaccine are immune to the virus for the rest of their lives. People who are infected with the virus and have the potential to spread it to others. Those who contracted the virus and recovered were immune to it for the rest of their lives. Figure (2.1) shows the flowchart diagram of the model, and how the proposed model divided the entire population size, T, into four disease stages: susceptible (S), vaccinated (V), infected (I), recovered (R), and the interaction between these four stages.

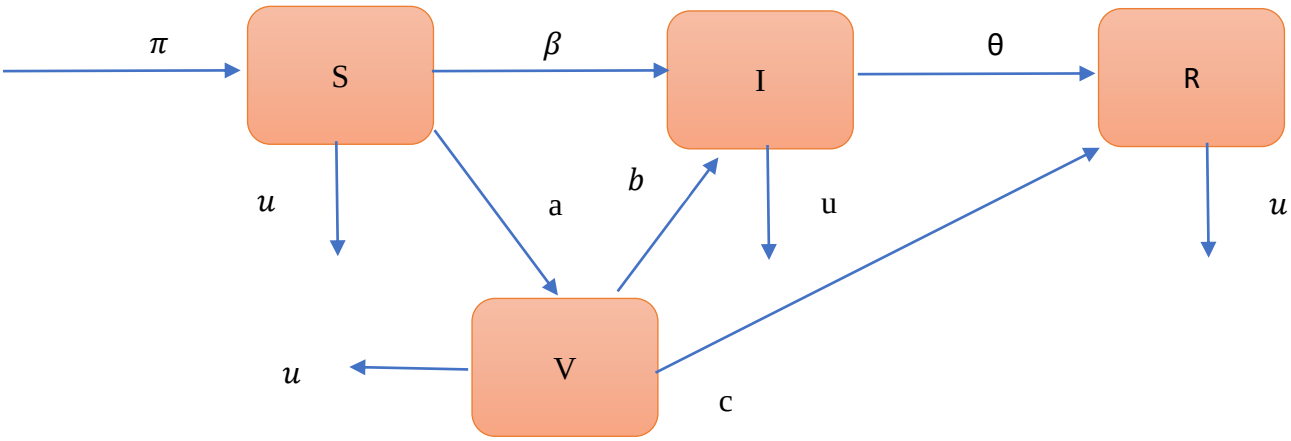

Figure 2.1: Flowchart diagram of the model

The following system of nonlinear ODEs is obtained by applying the Mass Action Law of infectious diseases to the Varicella epidemic in Jordan:

$$\begin{aligned} \frac{dS}{dt} &= \pi T - (u + a + \beta I)S, \\ \frac{dV}{dt} &= aS - (bI + c + u)V, \\ \frac{dI}{dt} &= \beta IS + bIV - (\theta + u)I, \\ \frac{dR}{dt} &= \theta I + cV - uR, \end{aligned} \tag{1}$$

and

$$T(t) = S(t) + V(t) + I(t) + R(t). \tag{2}$$

SVIR are the four compartments of the population (T), each of which is a function of time (t) that is determined by a system of differential equations. Tables (1) and (2) contain a list of all the definitions and descriptions of the variables and parameters utilized in the model.

Table 2.1 The model's variables

Variables	Descriptions
T	Number of total population
S	People who could contract the varicella virus
V	People who have received vaccinations
I	People infected with the varicella virus
R	People who have developed immunity and recovered from infections

Table 2.2 The model's parameters and their values

Parameters	Descriptions	
θ	The recovery rateThe rate of recovery	1/14
u	The rate of natural death	0.0019
π	Birth rate	0.03
a	The rate of vaccination among susceptible individuals	0.05
β	Disease transmission rate	0.24
c	The vaccine's effectiveness in preventing infection	0.92
b	The rate with which vaccinated individuals become vulnerable due to vaccine failure	0.08

3. Model Analysis

3.1 Positive Bounded Solutions and Positively Invariant Region

We explores how the proposed model might be applied in real-world scenarios with positive and bounded outcomes [27,28]. We have $\forall t \geq 0$:

We need to establish the norm:

$$\|Z\|_{\infty} = sup_{t \in D_Z} |Z(t)|. \tag{3}$$

Then

$$\begin{aligned}\frac{dS}{dt} &= \pi T - (u + a + \beta I)S,\\ &\geq -(u + a + \beta|I|)S,\\ &\geq -\left(u + a + \beta \ sup_{t\in D_I}|I|\right)S,\\ &= -(u + a + \beta \ \|I\|_\infty)S,\\ \Rightarrow S(t) &= S(0)\, e^{-(u+a+\beta\|I\|_\infty)t}, \qquad \forall t \geq 0.\end{aligned} \tag{4}$$

$$\begin{aligned}\frac{dV}{dt} &= aS - (bI + c + u)V,\\ &\geq -(b|I| + c + \mathrm{u})V,\\ &\geq -\left(b \ \ sup_{t\in D_I}|I| + c + u\right)V,\\ &= -(\ b\|I\|_\infty + c + u)V,\\ \Rightarrow V(t) &= V(0)\, e^{-(b\|I\|_\infty + c + \mathrm{u})t}, \qquad \forall t \geq 0.\end{aligned} \tag{5}$$

$$\begin{aligned}\frac{dI}{dt} &= \beta IS + bIV - (\theta + u),\\ &\geq -(\theta + u)I,\\ \Rightarrow I(t) &= I(0)\, e^{-(\theta+u)t}, \qquad \forall t \geq 0.\end{aligned} \tag{6}$$

$$\begin{aligned}\frac{dR}{dt} &= \theta I + cV - uR \ \geq -uR,\\ \Rightarrow I(t) &= I(0)\, e^{-(\theta+u)t}, \qquad \forall t \geq 0.\end{aligned} \tag{7}$$

Lemma 3.1 Assume that all the initial conditions are non-negative in R_+^4 for the system then the region $\Omega = \{\, (S,V,I,R) \in R_+^4 \,;\, S(t) \geq 0, V(t) \geq 0, I(t) \geq 0, R(t) \geq 0 \,\}$ is positively invariant.

Proof: From the given model equations, we have the followING

$$\begin{aligned}\left.\frac{dS}{dt}\right|_{S=0} &= \pi T \ \geq 0,\\ \left.\frac{dV}{dt}\right|_{V=0} &= aS \geq 0\,,\\ \left.\frac{dI}{dt}\right|_{I=0} &= 0,\end{aligned} \tag{8}$$

$$\left.\frac{dR}{dt}\right|_{R=0} = \theta I + cV \geq 0.$$

Therefore, the region Ω is positively invariant and model (1)'s solution will stay inside Ω.

3.2 Equilibrium Points and Qualitative analysis of the model

As we mentioned in equation (2), T(t) represents the total population of Jordan, which as of the end of 2021 was about 10,888,834 based on the Statistical Report of Communicable Diseases in Jordan. It is possible to rewrite each compartment as a proportion of the total population to obtain,

$$P_s(t) = \frac{S(t)}{T}, \qquad P_I(t) = \frac{I(t)}{T}, \qquad P_R(t) = \frac{R(t)}{T}, \; P_V(t) = \frac{V(t)}{T}, \quad . \tag{9}$$

$$P_T(t) = \frac{T(t)}{T} = P_s(t) + P_I(t) + P_V(t) + P_R(t) = 1. \tag{10}$$

E^*can be the equilibrium point of the SVIR model if $E^* = (P_S{}^*, P_V{}^*, P_I{}^*, P_R{}^*)$. This SVIR model system has two equilibrium points:

1. When $P_I = 0.$, E_0, The point of disease-free equilibrium (DFE) is attained.
2. When $P_I > 0$, E^* is the point of endemic equilibrium.

Assuming that there is no infection, we can replace $P_I = 0$ and $P_R = 0$ in system (1). Consequently, the DFE point, or infection free equilibrium, is

$$E_0 = \left(P_{S_0}, P_{V_0}, P_{R_0}, P_{I_0}\right) = \left(\frac{u}{(u+a)}, \; \frac{ua}{(u+a)(c+u)}, \; 0, 0\right). \tag{11}$$

Equations (1) will be utilized and solved for P_S in order to determine the system's second equilibrium point while presuming the presence of the virus.

$$P_S = \frac{u}{u+a+\beta P_I{}^*}, \tag{12}$$

Solve (1) for P_V to have,

$$P_V = \frac{au}{(bP_I{}^*+c+u)(u+a+\beta P_I{}^*)}, \tag{13}$$

Now, substitute (12) and (13) in (1), we have,

$$\frac{\beta u}{u+a+\beta P_I{}^*} + \frac{uba}{(u+a+\beta P_I{}^*)(bP_I{}^*+c+u)} - u - \theta = 0, \tag{14}$$

rearrange equation (14) in a quadratic equation form, to have,

$$K_1 P_I{}^{*2} + K_2 P_I{}^* + K_3(1-k) = 0, \tag{15}$$

where, $K_1 = b\beta(u+\theta) > 0, \qquad K_2 = (u+\theta)[b(u+a) + \beta(c+u)] - b\beta u,$

$$K_3 = (u+\theta)(u+a)(c+u) > 0, \quad k = \frac{u\beta}{(u+\theta)(u+a)} + \frac{uab}{(u+\theta)(u+a)(c+u)},$$

Then we get,

$$P_I{}^*{}_{1,2} = \frac{-K_2 \pm \sqrt{K_2{}^2 - 4K_1K_3(1-k)}}{2K_1}, \text{ then, } k > 1 \text{ and } P_I{}^* > 0$$

Consequently, the second equilibrium point of the system, sometimes referred to as the endemic equilibrium point, is

$$E^* = (P_S{}^*, P_V{}^*, P_I{}^*, P_R{}^*) = \left(\frac{u}{u+a+\beta P_I{}^*}, \frac{au}{(bP_I{}^*+c+u)(u+a+\beta P_I{}^*)}, P_I{}^*, 0\right).$$

(16)

3.3 Basic Reproduction Rate

In a population that is completely susceptible, the basic reproduction number (R_0)can be defined as the estimated number of secondary infections that a certain individual causes. By using (R_0), it is possible to accurately predict whether or not an infectious disease will spread throughout a population and cause a pandemic [29]. A few estimated basic reproduction rates are shown in table (3). Because of differences in population size rates, environmental influences, contact structure, and surrounds, different populations of people may be associated with different values of $(R_0)$for the same illness.

Table 3 The infectious disease's estimated (R_0) [30]

The disease	$(\boldsymbol{R_0})$
Rubella	6-7
Influenza	3-4
Chickenpox	10-12
Smallpox	3.5-6
The disease of Foot and mouth	3.6-4.6
Measles	16-18
Dengue	1.3-11.6

The Next Generation matrix is used to determine the fundamental reproduction number [31]. Any nonlinear ODE system was defined using this method as

$$z_i = f_i = F_i(z) - v_i(z), \tag{17}$$

and V_i can be expressed as

$$v_i = v_i(out) - v_i(in). \tag{18}$$

where F_I is the infection's rate to the i^{th} stage, $v_i(in)$ is the input rate for changing to i^{th} stage, $v_i(out)$ is the result rate of i^{th} stage, and if $F_i(z)$ is zero, the eigenvalues of the differentiation of $f(z_0)$, should be negative real ones.

Lemma 3.2 [32] Let the disease-free equilibrium point to be E_0 , then the differentiation of $F(x_0)$, and the differentiation of $v(x_0)$, could be written as:

$$F = \left[\frac{\partial f_i}{\partial z_j}(z_0)\right],\ v = \left[\frac{\partial v_i}{\partial z_j}(z_0)\right], j \le m\ and\ 1 \le i. \tag{19}$$

Therefore, the linearization of the SVIR model's ordinary differential equations is necessary for the differentiation of the fundamental reproduction number. Lemma (3.2) can be written as,

$$F = \begin{bmatrix} \beta P_{S_0} + bP_{V_0} & 0 \\ 0 & 0 \end{bmatrix}, \qquad V = \begin{bmatrix} \theta + u & 0 \\ 0 & bP_I + c + u \end{bmatrix}, \tag{20}$$

$$V^{-1} = \begin{bmatrix} \frac{1}{\theta+u} & 0 \\ 0 & \frac{1}{bP_I+c+u} \end{bmatrix}, \qquad FV^{-1} = \begin{bmatrix} \frac{\beta P_{S_0} + bP_{V_0}}{\theta+u} & 0 \\ 0 & 0 \end{bmatrix}, \tag{21}$$

To have two eigenvalues of the matrix FV^{-1}, that are $(0, \frac{\beta P_{S_0} + bP_{V_0}}{\theta+u})$.

$$R_0 = \rho[FV^{-1}] = \frac{\beta P_{S_0} + bP_{V_0}}{\theta+u}, \tag{22}$$

Let substitute P_{S_0} and P_{V_0} in equation (22) to have,

$$R_0 = \frac{\beta u}{(u+\theta)(u+a)} + \frac{uba}{(u+\theta)(u+a)(c+u)} = \frac{\beta u(c+u)+uba}{(u+\theta)(u+a)(c+u)}, \tag{23}$$

Which is similar to k value in (15), if $(R_0) < 1$, the infectious illness is under control and the disease is in the free stage; if $(R_0) > 1$, the virus is spreading and the pandemic is beginning.

3.4 Sensitivity Analysis of R_0

A specific parameter in λ can be used to generate R_0 using the normalized local sensitivity index, and this can be expressed as $\Omega_\lambda^{R_0} = \frac{\partial \boldsymbol{R_0}}{\partial \lambda}\frac{\lambda}{\boldsymbol{R_0}}$. With this updated definition, we can now

compute the indices below using table (2), which will provide R_0 for every parameter that appeared in [33].

.

$$\Omega_{\beta}^{R_0} = \frac{\partial \boldsymbol{R_0}}{\partial \beta}\frac{\beta}{\boldsymbol{R_0}} = \frac{u}{(u+\theta)(u+a)}\frac{\beta(u+\theta)(u+a)(c+u)}{\beta u(c+u)+uab} = \frac{\beta(c+u)}{\beta(c+u)+ba},$$

$$\Omega_{\theta}^{\boldsymbol{R_0}} = \frac{\partial \boldsymbol{R_0}}{\partial \theta}\frac{\theta}{\boldsymbol{R_0}} = \frac{-[\beta u(c+u)+uba](u+a)(c+u)}{[(u+a)(c+u))(\theta+u)]^2}\frac{\theta(u+\theta)(u+a)(c+u)}{\beta u(c+u)+uba} = \frac{-\theta}{(\theta+\mathrm{u})},$$

$$\Omega_{b}^{\boldsymbol{R_0}} = \frac{\partial \boldsymbol{R_0}}{\partial b}\frac{b}{\boldsymbol{R_0}} = \frac{(au)}{(u+\theta)(u+a)(c+u)}\frac{b(u+\theta)(u+a)(c+u)}{\beta u(c+u)+uba} = \frac{ab}{\beta(c+u)+ab},$$

$$\Omega_{u}^{\boldsymbol{R_0}} = \frac{\partial \boldsymbol{R_0}}{\partial u}\frac{u}{\boldsymbol{R_0}} = \frac{[\beta c+2\beta u+ab][(u+\theta)(u+a)(c+u)]+[-2cu-ca-\theta c-3u^2-2ua-2u\theta-\theta a][\beta u(c+u)+uba]}{(u+\theta)(u+a)(c+u)[\beta(c+u)+ab]},$$

$$\Omega_{c}^{\boldsymbol{R_0}} = \frac{\partial \boldsymbol{R_0}}{\partial c}\frac{c}{\boldsymbol{R_0}} = \frac{c[-uab]}{(c+u)[\beta u(c+u)+uab]}, \qquad \Omega_{a}^{\boldsymbol{R_0}} = \frac{\partial \boldsymbol{R_0}}{\partial a}\frac{a}{\boldsymbol{R_0}} = \frac{a[b(u+a)-\beta(c+u)-ab]}{(u+a)[\beta(c+u)+ab]},$$

As stated before, an infectious disease is vanishing if $R_0 < 1$ and spreading if $R_0 > 1$. The fundamental reproduction number R_0 is created using the next generation matrix, which served as our indication to assess the possibility for infectious diseases.

Using equation (22) and the number of actual cases listed in table (1), we may determine R_0 for the varicella virus in Jordan each year.

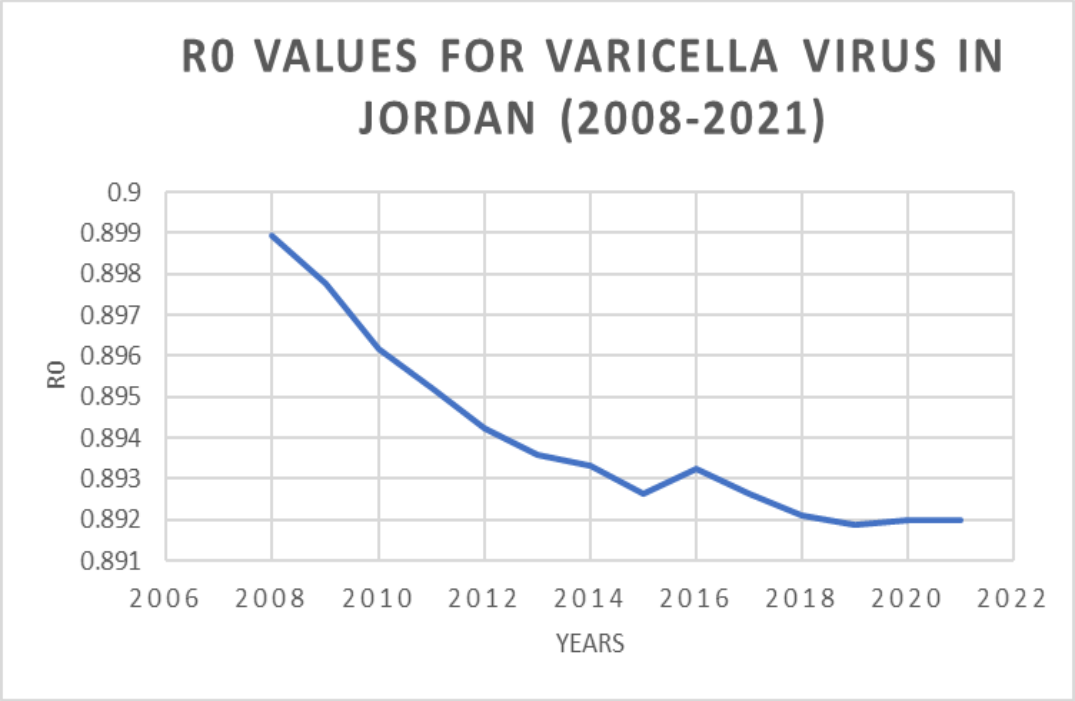

Figure 2: Jordan's varicella virus R_0 values from 2008 to 2021

The situation in Jordan was summarized in figure (2), which makes it clear that since 2016, there has been a significant drop in R_0 and that the number of cases has been brought under control. Jordanian health officials also publicly negotiated their strategies for combating infectious diseases from 2016 to 2020, which included adding more vaccinations, such as the varicella virus vaccine, to the country's national immunization program [34].

The varicella virus, a serious viral infection, is nevertheless highly transmissible. It is unclear how many instances there are of varicella in Jordan and what the statistics are. The local sensitivity analysis will be used to show how each and every parameter affects R_0. By replacing the parameters'amount from table (2) into the equations from (24) to (29), the sensitivity values can be found. The calculated sensitivity are shown in Table 4.

Table 4 Each parameter's sensitivity values in R_0

Sensitivity	$\Omega_{\beta}^{R_0}$	$\Omega_{u}^{R_0}$	$\Omega_{\theta}^{R_0}$	$\Omega_{a}^{R_0}$	$\Omega_{c}^{R_0}$	$\Omega_{b}^{R_0}$
Sinsitivity Values	0.98	0.59	-0.70	-0.61	-0.02	0.02

Table (4) allows us to determine how each parameter affects R_0. To begin, the transmission rate β shows that increasing it by, say, 10% will cause R_0 to grow by the same percentage, or 10%.

3.5 Existence and Uniqueness

By proving that the SVIR model's solutions exist and are unique, researchers can validate the model's , demonstrate the model's dependability, and enable in-depth analysis and prediction of infection dynamics within a population. They can also establish a strong mathematical basis for understanding the model. Consider the following form of the first-order ordinary differential equation:

$$z` = f(t, z), \qquad z(t_0) = z_0, \tag{24}$$

Let,

$$f_1 = u - (u + a + \beta P_I)P_S,$$
$$f_2 = aP_S - (bP_I + c + u)P_V,$$
$$f_3 = \beta P_I P_S + bP_I P_V - (\theta + u)P_I,$$

and

$$f_4 = \theta P_I + cP_V - uP_R\ .$$

We now have two theorems [35] that demonstrate the SVIR model's existence and uniqueness.

Theorem 3.1 (Uniqueness analysis of the solution)

Let T represents the domain, and $f(t,z)$ satisfies the Lipschitz condition, then

$$|t - t_0| \leq a\ , \|z - z_0 \leq b\ \|, z = (z, z, \dots, z_n), z_0 = (z_{10}, z_{20}, \dots, z_{n0}), \qquad (25)$$

and,

$$\|f(t, z_1) - f(t, z)\| \leq k\|z_1 - z_2\ \|, \qquad (26)$$

where (26) satisfies if,

$$\begin{cases}\frac{\partial f_i}{\partial z_j}, & i, j = 1,2, \dots, n\end{cases}$$

is bounded in the domain T and continuous.

Lemma 3.3

If the partial derivative of f(t,z) is continuous $\frac{\partial f_i}{\partial z_j}$, It satisfies a Lipschitz condition in R on a bounded closed convex domain of real number R.

Let the domain be,

$$1 \leq \delta \leq R, \qquad (27)$$

Afterward, if a bounded solution is discovered in the form of, $0 < R < \infty$.

Theorem 3.2 (Existence Analysis of the Solution)

In order for (26) and (27) to hold, let T represent the domain defined in (25) as follows. The model system of equations (1) then has a solution that is bounded in domain T.

Proof: Let,

$$f_1 = u - (u + a + \beta P_I)P_S, \quad (28)$$

$$f_2 = aP_S - (bP_I + c + u)P_V, \quad (29)$$

$$f_3 = \beta P_I P_S + bP_I P_V - (\theta + u)P_I \text{ , and} \quad (30)$$

$$f_4 = \theta P_I + cP_V - uP_R, \quad (31)$$

to show that $\frac{\partial f_i}{\partial z_j}$ are bounded and continuous, the partial derivatives will be determined. Take(28),

$\frac{\partial f_1}{\partial P_S} = -(u + a + \beta P_I),\ \left|\frac{\partial f_1}{\partial P_S}\right| = |-(u + a + \beta P_I)| < \infty,$

$\frac{\partial f_1}{\partial P_V} = 0,\ \left|\frac{\partial f_1}{\partial P_V}\right| = |0| < \infty,\ \frac{\partial f_1}{\partial P_I} = -\beta,\ \left|\frac{\partial f_1}{\partial P_V}\right| = |-\beta| < \infty, \frac{\partial f_1}{\partial P_R} = 0,\ \left|\frac{\partial f_1}{\partial P_R}\right| = |0| < \infty.$

Similarly, from equation (29), we get,

$\frac{\partial f_2}{\partial P_S} = a,\ \left|\frac{\partial f_2}{\partial P_S}\right| = |a| < \infty,\ \frac{\partial f_2}{\partial P_V} = -(bP_I + c + u),\ \left|\frac{\partial f_2}{\partial P_V}\right| = |-(bP_I + c + u)| < \infty,$

$\frac{\partial f_2}{\partial P_I} = -b,\ \left|\frac{\partial f_2}{\partial P_I}\right| = |-b| < \infty,\ \frac{\partial f_2}{\partial P_R} = 0,\ \left|\frac{\partial f_2}{\partial P_R}\right| = |0| < \infty.$

From (30), we havet,

$\frac{\partial f_3}{\partial P_S} = \theta P_I,\ \left|\frac{\partial f_3}{\partial P_S}\right| = |\beta P_I| < \infty, \frac{\partial f_3}{\partial P_V} = bP_I,\ \left|\frac{\partial f_3}{\partial P_V}\right| = |bP_I| < \infty,$

$\frac{\partial f_3}{\partial P_I} = \beta P_S + bP_V + -(\theta + u)\ ,\ \left|\frac{\partial f_3}{\partial P_I}\right| = |\beta P_S + bP_V + -(\theta + u)\ | < \infty,$

$\frac{\partial f_3}{\partial P_R} = 0,\ \left|\frac{\partial f_3}{\partial P_R}\right| = |0| < \infty.$

From equation (31), to have,

$\frac{\partial f_4}{\partial P_S} = 0,\ \left|\frac{\partial f_4}{\partial P_S}\right| = |0| < \infty,\ \frac{\partial f_4}{\partial P_V} = c,\ \left|\frac{\partial f_4}{\partial P_V}\right| = |c| < \infty,$

$\frac{\partial f_4}{\partial P_I} = \theta,\ \left|\frac{\partial f_4}{\partial P_I}\right| = |\theta| < \infty,\ \frac{\partial f_4}{\partial P_R} = -u,\ \left|\frac{\partial f_4}{\partial P_R}\right| = |-u| < \infty.$

The domain T has a single solution to the model system of equations (1), as a result of the theorem (3.1), which makes it evident that all of the partial derivatives are bounded and continuous.

4. Analysis of the Stability of the Model

We must specify the approach we will take in order to investigate the stability of the two equilibrium points of the SVIR model, which contains nonlinear differential equations. According to the Hartman-Grobman theorem, a continuous function with a continuous inverse in the vicinity of this point into R^n exists if the linearization of the equations' solution has neither zero nor imaginary eigenvalues.

Thus, Jacobian matrix can be written for (P_S, P_V, P_I) to be

$$J = \begin{bmatrix} -(u + a + \beta P_I) & 0 & -\beta P_S \\ a & -(bP_I + c + u) & -bP_V \\ \beta P_I & bP_I & \beta P_S + bP_V - \theta - u \end{bmatrix}. \quad (32)$$

4.1 Local Stability of DFE

The disease-free equilibrium point (DFE), gives

$$J = \begin{bmatrix} -(u + a) & 0 & -\beta P_S \\ a & -(c + u) & -bP_V \\ 0 & 0 & \beta P_S + bP_V - \theta - u \end{bmatrix}. \quad (33)$$

We can state that the DFE point is locally asymptotically stable if we demonstrate that the eigenvalues of the Jacobian matrix contain a negative real portion [36]. We discovered three DFE eigenvalues using Maple program, which are

$$\lambda_1 = -(c + u),$$
$$\lambda_2 = -(u + a),$$
$$\lambda_3 = \beta P_S + bP_V - \theta - u,$$

It is found that λ_1 and λ_2 have negative real values. Now we have to check λ_3 and check if it is negative, it means our DFE is locally stable.

$$\beta P_S + bP_V - \theta - u < 0,$$
$$\beta P_S + bP_V < \theta + u,$$
$$\frac{\beta P_S + bP_V}{\theta + u} < 1,$$

which is the same value of R_0, that means, $R_0 < 1$, Consequently, we can declare our system to be locally stable, when $P_I = 0$. While if $R_0 > 1$, then E_0 is unstable.

4.2 Local Stability of the Endemic Point ((Routh-Hurwitz stability criterion)

Apply this matrix now to the system's second equilibrium point, also known as the endemic equilibrium point, as shown in equation 3.25 to obtain,

$$J = \begin{bmatrix} -(u + a + \beta P_I^*) & 0 & -\beta P_S \\ a & -(bP_I^* + c + u) & -bP_V \\ \beta P_I^* & bP_I^* & \beta P_S + bP_V - \theta - u \end{bmatrix}, \quad (34)$$

By rearranging the parameters elements in a_{ii} in the matrix (34) [37] then, we have:

$$-(u + a + \beta P_I) = \frac{-u}{P_S^*},$$

$$-\left(bP_I{}^* + c + u\right) = \frac{-aP_S{}^*}{P_V{}^*},$$

Thus, $\beta P_S + bP_V - \theta - u = 0$.

Then, we get,

$$J = \begin{bmatrix} \frac{-u}{P_S{}^*} & 0 & -\beta P_S{}^* \\ a & \frac{-aP_S{}^*}{P_V{}^*} & -bP_V{}^* \\ \beta P_I{}^* & bP_I{}^* & 0 \end{bmatrix}. \quad (35)$$

Then,

$q(\lambda) = \lambda^m + a_1\lambda^{m-1} + \cdots + a_m$, where a_i represents all the real coefficients for all $i = 1,2,3,\ldots,m$. When q(λ)=0, the roots of this polynomial are all negative or have a negative real component if and only if every Routh-Hurwitz matrix's determinant is nonnegative [38]. The following outcomes are obtained by applying the Routh-Hurwitz stability equation and theorem 3.6:

The characteristic equation for (35) matrix is,

$$\lambda^3 + c_1\lambda^2 + c_2\lambda + c_3 = 0,$$

where,

$$c_1 = \frac{u}{P_S{}^*} + \frac{aP_S{}^*}{P_V{}^*} > 0, \qquad c_2 = \frac{aP_S{}^*}{P_V{}^*} + a^2P_V{}^*P_I{}^* + \beta^2P_S{}^*P_I{}^* > 0,$$

$$c_3 = ab\beta P_S{}^*P_I{}^* + \frac{a\beta^2P_I{}^*P_S{}^{*2}}{P_V{}^*} + \frac{ub^2P_V{}^*P_I{}^*}{P_S{}^*} > 0,$$

now, if $c_1c_2 - c_3 > 0$, In order to verify that the endemic equilibrium point is locally stable according to the Routh-Hurwitz stability criterion, we substitute the final inequality to have:

$$\frac{au^2}{P_S{}^*P_V{}^*} + (u + \beta P_I{}^*)\beta^2P_I{}^*P_S{}^* + \frac{a^2uP_S{}^*}{P_V{}^{*2}} + bP_I{}^*P_S{}^*(\beta - b)^2 + ab\beta P_S{}^*P_I{}^* > 0.$$

Then, the endemic equilibrium point is stable

4.3 Global stability using Lyapunov for Disease-free Equilibrium

Theorem 4.1. [34] When the reproductive number $R_0 < 1$, the system is globally asymptotically stable at DFE, while the reproductive number $R_0 > 1$ makes the system globally asymptotically unstable at DFE.

Proof: Think about the Lyapunov function in this way:

$W(S^*, C^*, J^*, H^*) = (S - S^* - S^*\log\frac{S^*}{S}) + (V - V^* - V^*\log\frac{V^*}{V}) + I + R.$

(36)

The following outcome is obtained by applying the derivative with regard to t on both sides:

$$\frac{dW}{dt} = \left(1 - \frac{S^*}{S}\right)\frac{dS}{dt} + \left(1 - \frac{V^*}{V}\right)\frac{dV}{dt} + \frac{dI}{dt} + \frac{dR}{dt} \quad . \tag{37}$$

At this point, their derivative values can be used as follows:

$$\frac{dW}{dt} = \left(1 - \frac{S^*}{S}\right)[\pi N - (u + a + \beta I)S] + \left(1 - \frac{V^*}{V}\right)[aS - (bI + c + u)V]$$
$$+[\beta IS + bIV - (\theta + u)I] + [\theta I + cV - uR]. \tag{38}$$

Putting $S = S - S^*,\ V = V - V^*,\ I = I - I^*,\ R = R - R^*$.

$$\frac{dW}{dt} = \left(1 - \frac{S^*}{S}\right)[\pi N - (u + a + \beta(I - I^*))(S - S^*)]$$
$$+ \left(1 - \frac{V^*}{V}\right)[aS - (b(I - I^*) + c + u)(V - V^*)]$$
$$+[\beta IS + bIV - (\theta + u)I](I - I^*) + [\theta(I - I^*) + c(V - V^*) - u(R - R^*)]. \tag{39}$$

After some computations, we have

$$\frac{dW}{dt} = \pi N - \pi N\frac{S^*}{S} - (u + a + \beta(I - I^*))\frac{(S - S^*)^2}{S} + aS - aS\frac{V^*}{V}$$
$$-(b(I - I^*) + c + u)\frac{(V - V^*)^2}{V} + \beta(I - I^*)(S - S^*) + b(I - I^*)(V - V^*)$$
$$-(\theta + u)(I - I^*) + \theta(I - I^*) + c(V - V^*) - u(R - R^*).$$

From above equation, $\frac{dW}{dt} < 0$ for $R_0 < 1$.

If $S = S^*,\ V = V^*,\ I = I^*,\ R = R^*$, then $\frac{dW}{dt} = 0$

Consequently, it may be said that proposed system is globally asymptotically stable at DFE.

4.4 Global stability using Lyapunov for Endemic Equilibrium

All of the independent variables in the model are set using the endemic Lyapunov function; in this instance, $L(S^*, V^*, I^*, R^*)$, L < 0 represents an adverse equilibrium.

Theorem 4.2. [34] When the reproductive number $R_0 > 1$, the system is globally asymptotically stable at endemic equilibrium, while the reproductive number $R_0 < 1$ makes the system globally asymptotically unstable at endemic equilibrium.

Proof: Think about the Lyapunov function in this way:

$$L(S^*, C^*, J^*, H^*)$$
$$= (S - S^* - S^*\log\frac{S^*}{S}) + (V - V^* - V^*\log\frac{V^*}{V}) + \left(I - I^* - I^*\log\frac{I^*}{I}\right) + \left(R - R^* - R^*\log\frac{R^*}{R}\right).$$

(40)

Applying the derivative with respect to t on both sides yields the following result:

$$\frac{dL}{dt} = \left(1 - \frac{S^*}{S}\right)\frac{dS}{dt} + \left(1 - \frac{V^*}{V}\right)\frac{dV}{dt} + \left(1 - \frac{I^*}{I}\right)\frac{dI}{dt} + \left(1 - \frac{R^*}{R}\right)\frac{dR}{dt}. \quad (41)$$

At this point, their derivative values can be used as follows:

$$\frac{dL}{dt} = \left(1 - \frac{S^*}{S}\right)[\pi N - (u + a + \beta I)S] + \left(1 - \frac{V^*}{V}\right)[aS - (bI + c + u)V]$$
$$+ \left(1 - \frac{I^*}{I}\right)[\beta IS + bIV - (\theta + u)I] + \left(1 - \frac{R^*}{R}\right)[\theta I + cV - uR]. \quad (42)$$

Putting $S = S - S^*,\ V = V - V^*,\ I = I - I^*,\ R = R - R^*$.

$$\frac{dL}{dt} = \left(1 - \frac{S^*}{S}\right)[\pi N - (u + a + \beta(I - I^*))(S - S^*)] + \left(1 - \frac{V^*}{V}\right)[aS - (b(I - I^*) + c + u)(V - V^*)]$$
$$+ \left(1 - \frac{I^*}{I}\right)[\beta(S - S^*) + b(V - V^*) - (\theta + u)](I - I^*)]$$
$$+ \left(1 - \frac{R^*}{R}\right)[\theta(I - I^*) + c(V - V^*) - u(R - R^*)]. \quad (43)$$

$$\frac{dL}{dt} = \pi N - \pi N\frac{S^*}{S} - (u + a + \beta(I - I^*))\frac{(S - S^*)^2}{S} + aS - aS\frac{V^*}{V} - (b(I - I^*) + c + u)\frac{(V - V^*)^2}{V}$$
$$+\beta(S - S^*)\frac{(I - I^*)^2}{I} + b(V - V^*)\frac{(I - I^*)^2}{I} - (\theta + u)\frac{(I - I^*)^2}{I} + \theta(I - I^*) - \theta(I - I^*)\frac{R^*}{R} +$$
$$c(V - V^*) - c(V - V^*)\frac{R^*}{R} - u\frac{(R - R^*)^2}{R}. \quad (44)$$

To make things simpler, we may rephrase the relation above like this:

$$\frac{dL}{dt} = \Psi - \Upsilon. \quad (45)$$

$$\Psi = \pi N + aS + \beta(S - S^*)\frac{(I - I^*)^2}{I} + b(V - V^*)\frac{(I - I^*)^2}{I} + \theta(I - I^*) + c(V - V^*).$$

$$\Upsilon = \pi N\frac{S^*}{S} + (u + a + \beta(I - I^*))\frac{(S - S^*)^2}{S} + aS\frac{V^*}{V} + (b(I - I^*) + c + u)\frac{(V - V^*)^2}{V}$$
$$+(\theta + u)\frac{(I - I^*)^2}{I} + \theta(I - I^*)\frac{R^*}{R} + c(V - V^*)\frac{R^*}{R} + u\frac{(R - R^*)^2}{R}.$$

If $\Psi < \Upsilon$ then $\frac{dL}{dt} < 0$.

If $S = S^*,\ V = V^*,\ I = I^*,\ R = R^*$ then

$$\Psi - \Upsilon = 0 \ \Rightarrow \frac{dL}{dt} = 0.$$

For the proposed model, we deduce that the biggest compact invariant collection in

$$\left\{(S^*, V^*, I^*, R^*) \in \varpi: \frac{dL}{dt} = 0\right\}. \quad (46)$$

is the considered model's endemic equilibrium. We can deduce that endemic equilibrium is globally asymptotically stable using Lasalle's invariance idea if $\Psi < \Upsilon$.

5. Resutls and Discussion

Although the situation is different for the recovery rate θ and the vaccination rate for the susceptible a, we can observe that a 10% rise in θ and a will cause R_0 to drop by 7.04% and 6.08%, respectively, which makes sense. R_0 will rise by 0.20% for the parameter α, which measures the rate at which vaccinated individuals contract the virus due to vaccination failure, and fall by 0.17% for the parameter c, which measures the rate at which vaccination confers immunity from the virus. R_0will rise by 5.91% if u is increased by 10%. Figures (3)–(8) provide a graphic representation of the parameters.

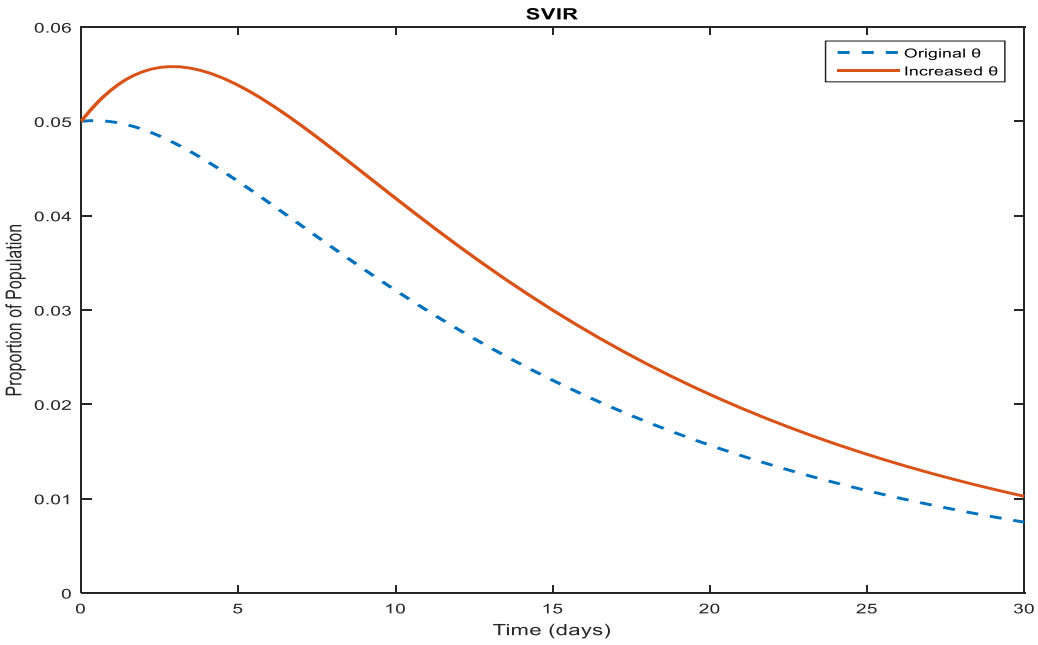

Figure 3: Varicella virus-infected individuals percentage as calculated by the model using the initial θ value in Table (3) and a 10% increase in the θ parameter.

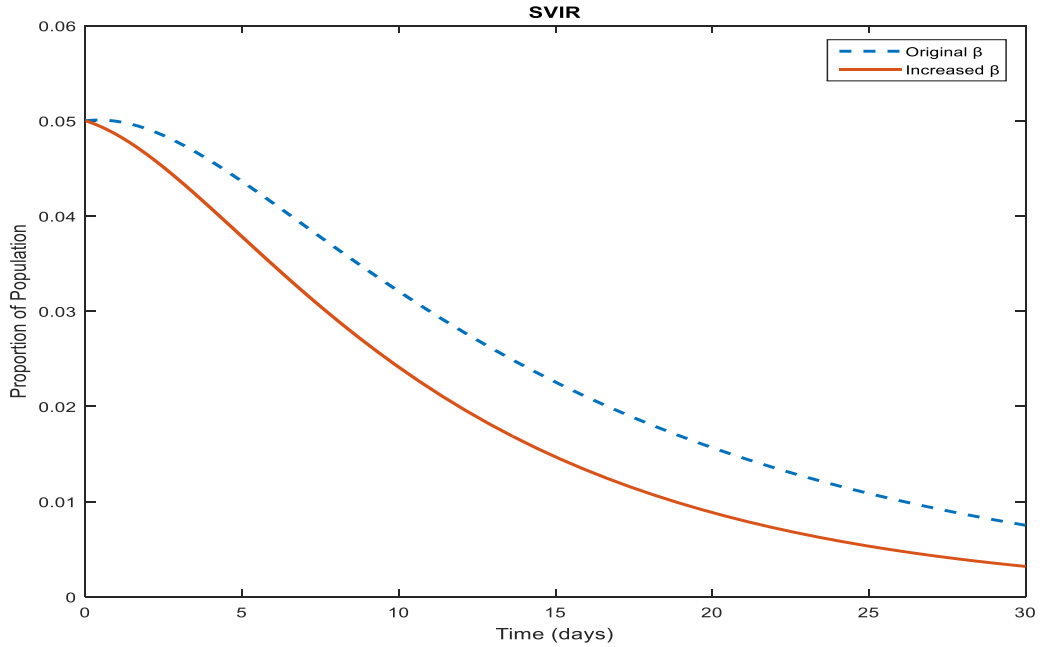

Figure 4: The model calculated the rate of the individuals infected with the varicella virus using the original β value in Table (3) and an increase of 10% in the β parameter.

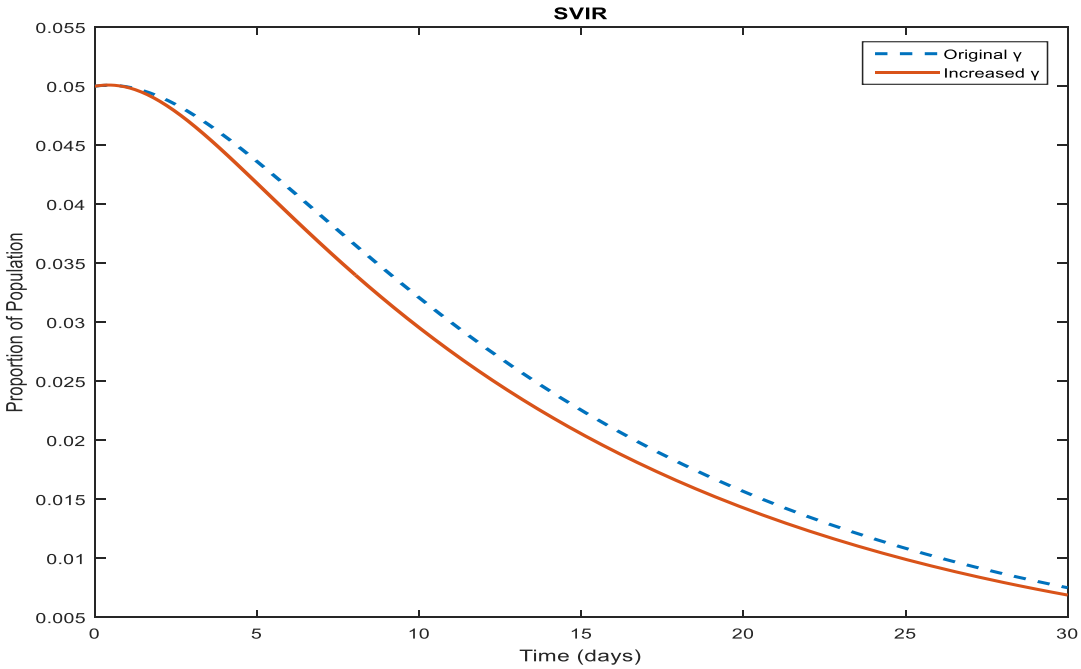

Figure 5: The model predicted the rate of the individuals infected with the varicella virus using the original γ value in Table (3) and increasing the γ parameter by 10%.

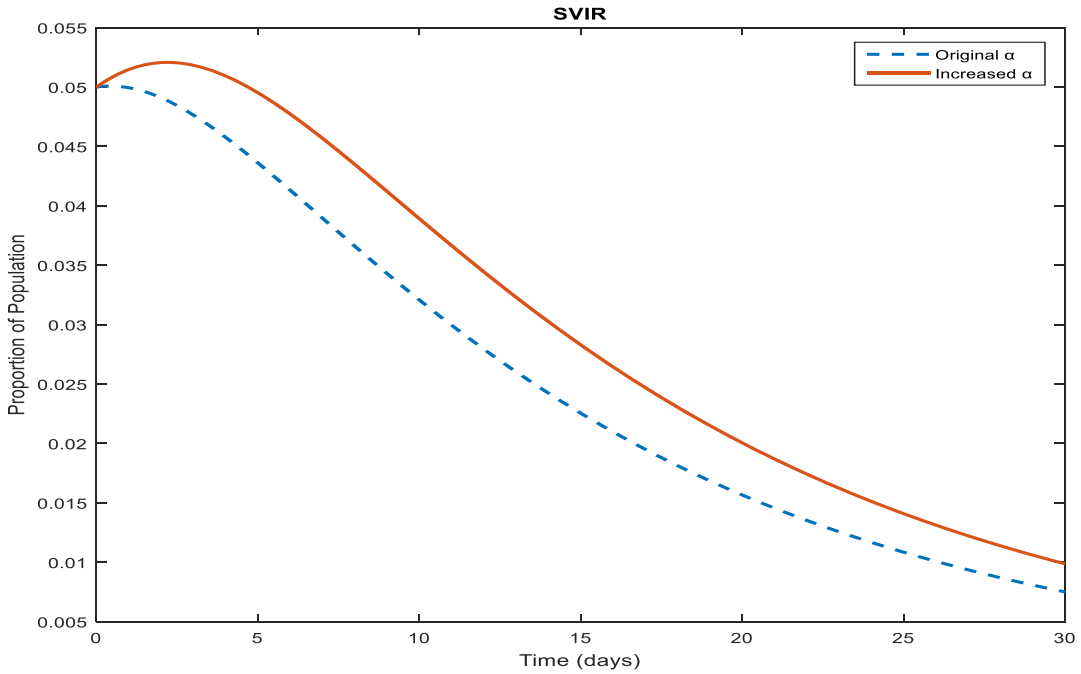

Figure 6: The model calculated the rate of the individuals infected with the varicella virus using the original α value in Table (3) and an increase of 10% in the α parameter.

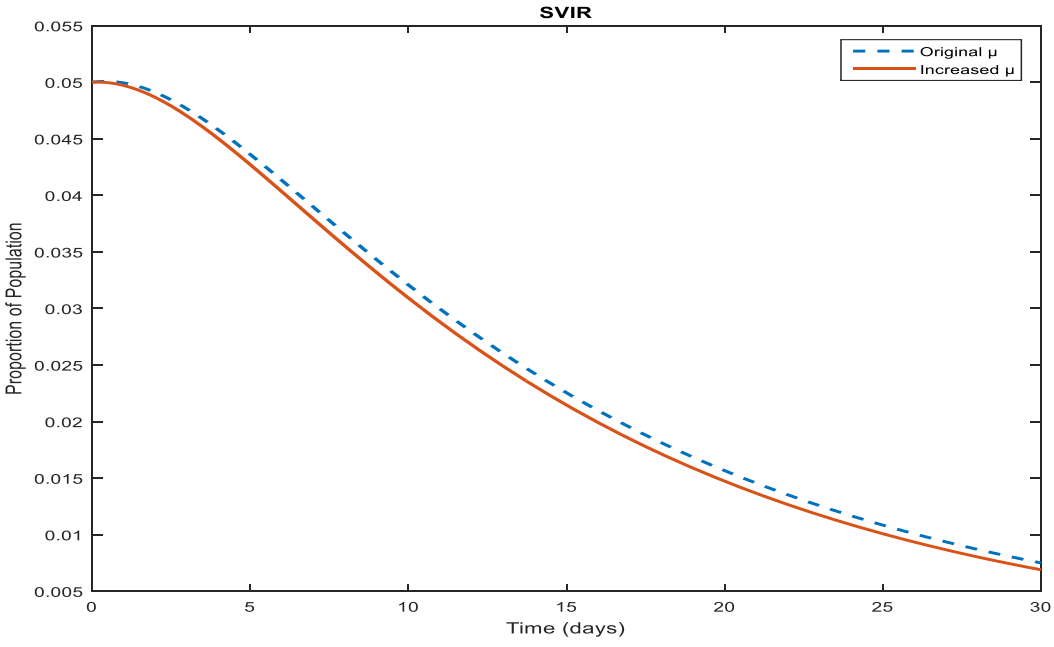

Figure 7: The model predicted the rate of the individuals infected with the varicella virus using the original μ value in Table (3) and increasing the μ parameter by 10%.

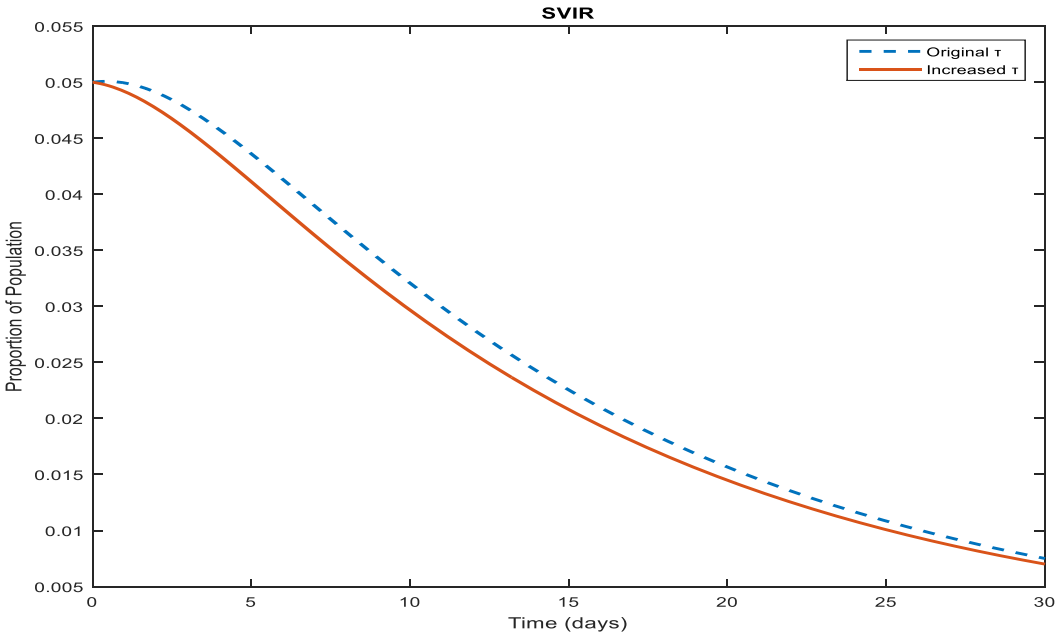

Figure 8: The model predicted the rate of the individuals infected with the varicella virus using the original τ value in Table (3) and increasing the τ parameter by 10%.

We examined the impact of the parameter on the percentage of the individuals that infected by the virus, as shown in the preceding graphs, and the outcomes of the system simulation matched the figures computed in table (4). Beginning with the impact of raising the transmission rate by 10%, as shown in the graph that the rate of infection grows as a result of this change in figure (3). Additionally, figure (6) illustrates how the infection would increase if the vaccine failure increases. Conversely, as illustrated in figures (4) and (5), a rise in the recovery and immunization rates will reduce the spread of infection among people.

In addition to these two factors, figure (8) shows a graph that illustrates if vaccinations are successful in providing immunity and whether inter-individual infection will decrease if the rate of transfer from the immunization compartment to the recovery compartment increases. Sensitivity analysis, which evaluates how parameter changes impact the model's output and offers insights into the model's robustness and dependability, is essential to this model for the SVIR of varicella virus. Finding the parameter that has the biggest influence on the model's output is one of these functions. Professionals can concentrate on accurately identifying or assessing this crucial element.

Sensitivity analysis is frequently used within the context of the SVIR model to pinpoint characteristics that significantly affect the dynamics of the varicella virus disease. These factors include the availability of vaccinations, their efficiency, the length of immunity, and the frequencies of interactions.

Table (2), includes parameter values for the SVIR model's set of equations in (1), will be used in the model simulation. It takes into account the state of infection in Jordan as well as the manner in which individuals move from susceptible, vaccinated, or infected to recovered. We began our model with the assumption that the population will transition from a disease-free state to one of endemicity.

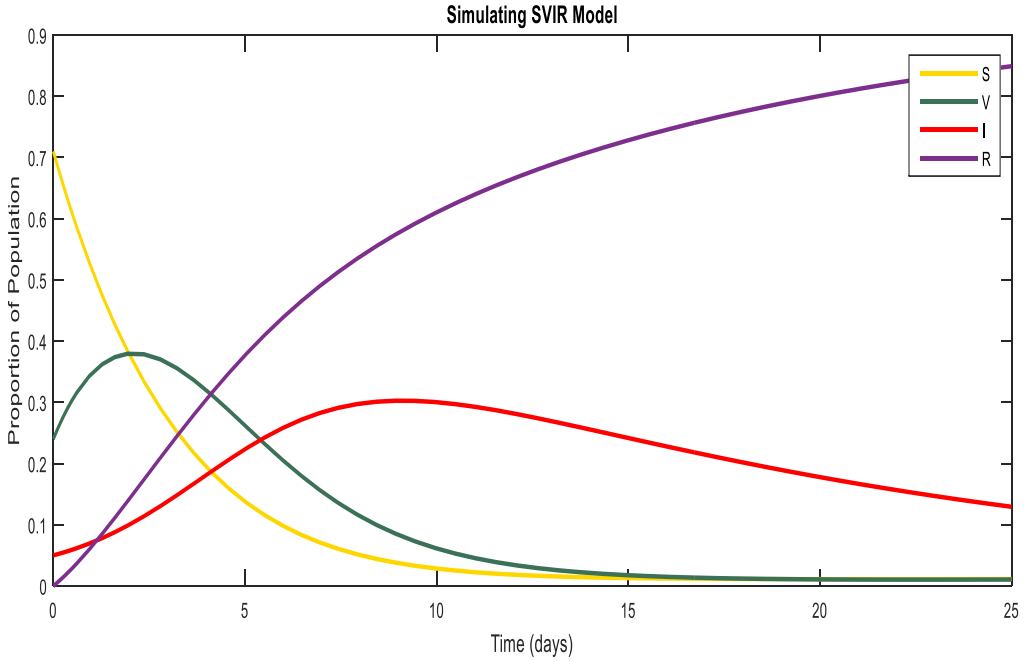

Figure 9: During the outbreak, different compartments' dynamics with $P_{V_0} = 0.24$

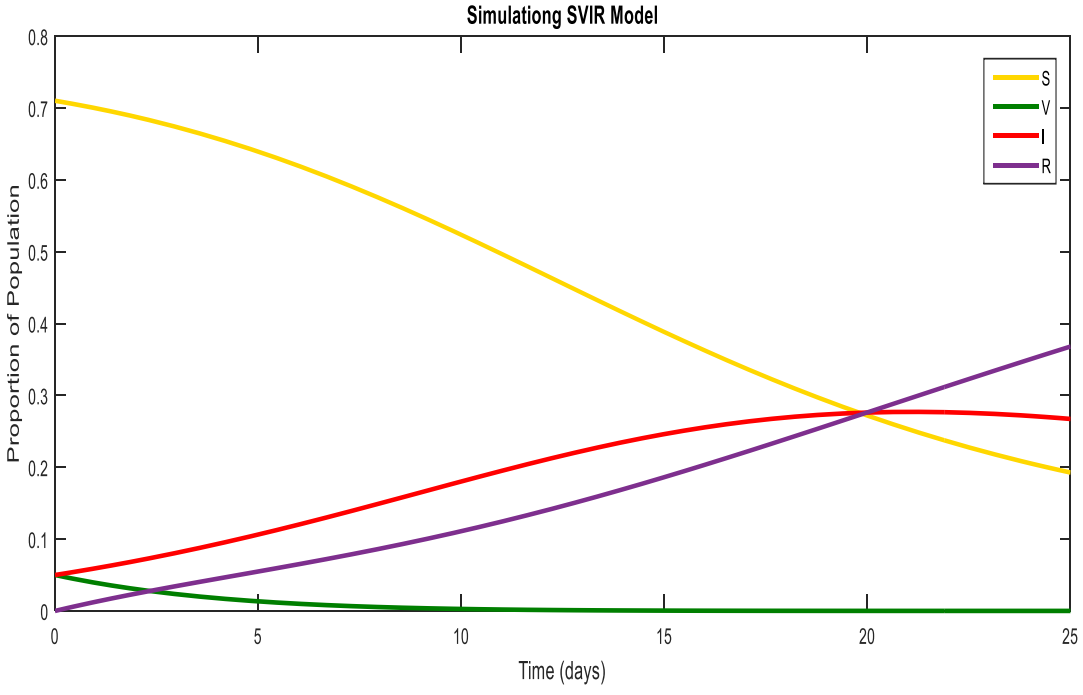

Figure 10: The several compartments' dynamics during the outbreak with $P_{V_0} = 0.05$

When the initial proportion of diseased people is 0.05 and the vaccination rate is 0.24, as shown in Figure (9), As we take the beginning value of 0.71, it is evident that the percentage of susceptible individuals begins to decline over time, while the infected ratio begins to rise and the individuals move to the recovery compartment over time. In contrast, the vaccination rate drops to 0.05 in figure (10) while the proportion of diseased people remains constant. As a result, in comparison to graph (9), the number of infected cases increases quickly over time. The number of recovered people rises as a result of people continuously migrating from the infected compartment to the recovered. Both figures demonstrate how vaccination-susceptible individuals might lessen the spread of the virus and, consequently, the total burden of illness. People can avoid contracting the varicella virus and developing health issues by being vaccinated. Long-lasting protection from varicella immunization reduces the likelihood of epidemics and fosters community health.

Reducing the overall burden of varicella virus infection allows for more money to be allocated to other health issues. Additionally, by assessing how parameter changes affect the effectiveness of control techniques, sensitivity analysis helps to achieve the best possible performance of therapies. By looking at how changes to important parameters impact the outcomes of vaccine schedules, extra doses, or particular therapies, policymakers can identify the most important aspects and develop policies that significantly reduce the incidence of varicella.

6. Conslusion

The dynamics of the SVIR model are examined in this study, and the model's numerical simulation was supplied. The equilibrium points of the model were identified, as well as the existence and uniqueness of the model's solution, local stability, and the basic reproduction number R_0. Existence and individuality Proofs confirm that the model's predictions are accurate and useful for decision-making. We discovered that the endemic equilibrium point is constant and that disease is consistently present amongst individuals when R_0>1.

Nonetheless, it is shown that when R_0 <1, the disease-free equilibrium is preserved. Here, vaccination acceptance, adherence to control measures, and varicella prevention measures

will all be aided by public health awareness campaigns, educational programs, and behavioural interventions. The ability to handle varicella patients and the possible burden on healthcare systems during outbreaks will also be evaluated, if needed, using the healthcare resources, such as hospital beds and medical staff. By altering the parameter values while holding all other health-related variables constant, we were able to evaluate the sensitivity of $R_0$and provide a visual description of it.

In the SVIR model of the varicella virus, sensitivity analysis of R_0 is crucial. It helps determine important parameters, evaluate model adaptability, and increase the efficacy of intervention strategies. Researchers can better understand the dynamics of infectious illnesses, evaluate the potential effects of different control measures, and influence public health initiatives to slow the spread of disease by doing sensitivity analysis of R_0 in the SVIR model. In conclusion, it should be noted that the SVIR model does not take into consideration changes in population size or demographic composition brought about by immigration and Fixed assumptions cannot completely convey the complications introduced by real-world vaccination rates and coverage. By doing so, disease dynamics can be more accurately represented, and better forecasts and policy recommendations can be made.

Since the varicella virus places a significant strain on the nation's healthcare system, the Jordanian Ministry of Health should set up vaccination campaigns to eradicate the illness. This is because a universal varicella vaccination is required. Long-lasting protection from varicella immunization reduces the likelihood of epidemics and fosters community health. Reducing the overall burden of varicella virus infection allows for more money to be allocated to other health issues. By using fractional-order differential equations instead of regular differential equations, we can simulate real-world processes while reducing the inaccuracies brought on by the missing parameters. Finally, more research is recommended, especially for diverse and non-constant populations. With the information acquired from this study, governments and medical organizations may create effective plans that lessen the effects of the varicella virus and protect individuals who are most impacted.

Data Availablity: All data available in manuscript.

Conflicts of Intrest: On behalf of all authors, the corresponding author states that there is no conflict of interest.

References:

[1]. Pergam, S. A., Limaye, A. P., & AST Infectious Diseases Community of Practice. (2009). Varicella zoster virus (VZV). American journal of transplantation: official journal of the American Society of Transplantation and the American Society of Transplant Surgeons, 9(Suppl 4), S108.

[2]. Gershon, A. A., & Silverstein, S. J. (2009). Varicella-zoster virus. Clinical virology, 451-474.

[3]. Thandi, C. S., & Whittam, L. (2021). Diagnosis and management of common viral skin infections. Prescriber, 32(4), 10-14.

[4]. Gilden, D., Cohrs, R. J., Mahalingam, R., & Nagel, M. A. (2009). Varicella zoster virus vasculopathies: diverse clinical manifestations, laboratory features, pathogenesis, and treatment. The Lancet Neurology, 8(8), 731-740.

[5]. World Health Organization. (2014). Varicella and herpes zoster vaccines: WHO position paper, June 2014. Weekly Epidemiological Record= Relevé épidémiologique hebdomadaire, 89(25), 265-287.

[6]. Papaloukas, O., Giannouli, G., & Papaevangelou, V. (2014). Successes and challenges in varicella vaccine. Therapeutic advances in vaccines, 2(2), 39-55.

[7]. Vázquez, M., LaRussa, P. S., Gershon, A. A., Niccolai, L. M., Muehlenbein, C. E., Steinberg, S. P., & Shapiro, E. D. (2004). Effectiveness over time of varicella vaccine. Jama, 291(7), 851-855.

[8]. Freer, G., & Pistello, M. (2018). Varicella-zoster virus infection: natural history, clinical manifestations, immunity and current and future vaccination strategies. New Microbiologica, 41(2), 95-105.

[9]. Trauer, J. M., Denholm, J. T., & McBryde, E. S. (2014). Construction of a mathematical model for tuberculosis transmission in highly endemic regions of the Asia-Pacific. Journal of theoretical biology, 358, 74-84.

[10]. Tabassum, M. F., Saeed, M., Akgül, A., Farman, M., & Chaudhry, N. A. (2020). Treatment of HIV/AIDS epidemic model with vertical transmission by using evolutionary Padé-approximation. Chaos, Solitons & Fractals, 134, 109686.

[11]. Adiga, A., Dubhashi, D., Lewis, B., Marathe, M., Venkatramanan, S., & Vullikanti, A. (2020). Mathematical models for covid-19 pandemic: a comparative analysis. Journal of the Indian Institute of Science, 100(4), 793-807.

[12]. Tabassum, M. F., Akgul, A., Akram, S., Farman, M., Karim, R., & Hassan, S. M. U. (2022). Treatment of dynamical nonlinear Measles model: An evolutionary approach. International Journal of Nonlinear Analysis and Applications, 13(1), 1629-1638.

[13]. Avwerosuo, A. A., & Okedoye, A. M. (2023). Mathematical Modelling of the Dynamics and Control of Communicable Diseases with Emphasis on Cholera Epidemics. Asian Journal of Applied Science and Technology (AJAST), 7(4), 99-119.

[14]. Xu, C., & Farman, M. (2023). Dynamical transmission and mathematical analysis of Ebola virus using a constant proportional operator with a power law kernel. Fractal and Fractional, 7(10), 706.

[15]. Karhunen, M., Leino, T., Salo, H., Davidkin, I., Kilpi, T., & Auranen, K. (2010). Modelling the impact of varicella vaccination on varicella and zoster. Epidemiology & Infection, 138(4), 469-481.

[16]. Edward, S., Kuznetsov, D., & Mirau, S. (2014). Modeling and stability analysis for a varicella zoster virus model with vaccination. Applied and Computational Mathematics, 3(4), 150-162.

[17]. Talbird, S. E., La, E. M., Mauskopf, J., Altland, A., Daniels, V., & Wolfson, L. J. (2018). Understanding the role of exogenous boosting in modeling varicella vaccination. Expert Review of Vaccines, 17(11), 1021-1035.

[18]. Horn, J., Damm, O., Greiner, W., Hengel, H., Kretzschmar, M. E., Siedler, A., ... & Mikolajczyk, R. T. (2018). Influence of demographic changes on the impact of vaccination against varicella and herpes zoster in Germany–a mathematical modelling study. BMC medicine, 16, 1-9.

[19]. Suh, J., Choi, J. K., Lee, J., & Park, S. H. (2022). Estimation of single-dose varicella vaccine effectiveness in South Korea using mathematical modeling. Human Vaccines & Immunotherapeutics, 18(5), 2085468.

[20]. Annual Statistical Report of Communicable Diseases. (2021). Communicable Diseases, Pages 12, 189-196 Directorate. https://moh.gov.jo/EchoBusV3.0/SystemAssets/Communicable/Annual%20report%202021.pdf

[21]. Alfauri, M. A., Mohammad, A. I., Aqel, A. J., & Asad, M. (2022). Trend of Chickenpox in Jordan (2013-2020). Iproceedings, 8(1), e36589.

[22]. Liu, X., Takeuchi, Y., & Iwami, S. (2008). SVIR epidemic models with vaccination strategies. Journal of Theoretical biology, 253(1), 1-11.

[23]. Centers for Disease Control and Prevention (CDC). (2021). National Center for Immunization and Respiratory Diseases (NCIRD), Division of Viral Diseases.

[24]. https://www.cdc.gov/chickenpox/about/transmission.html#:~:text=The%20virus%20spreads%20easily%20from,with%20someone%20who%20has%20chickenpox.

[25]. Steiner, K., Wallrafen, N., & Weiss, D. (2018). Development of a Mathematical Model of the Spread of Chicken Pox in a Contained Population.

[26]. Kirwa, P., Rotich, T., Obogi, R., & Tanui, P. K. (2017). Boundedness and positivity of a mathematical model of the immune response to HIV infection. Int. J. Sci. Res. Eng. Tech., 6, 847-849.

[27]. Zephaniah, O. C., Nwaugonma, U. I. R., Chioma, I. S., & Adrew, O. (2020). A mathematical model and analysis of an SVEIR model for streptococcus pneumonia with saturated incidence force of infection. Mathematical Modelling and Applications, 5(1), 16-38.

[28]. Diekmann, O., Heesterbeek, J. A. P., & Metz, J. A. (1990). On the definition and the computation of the basic reproduction ratio R 0 in models for infectious diseases in heterogeneous populations. Journal of mathematical biology, 28, 365-382.

[29]. Rodrigues, H. S. F. (2012). Optimal control and numerical optimization applied to epidemiological models (Doctoral dissertation, Universidade de Aveiro (Portugal)).

[30]. Diekmann, O., Heesterbeek, J. A. P., & Roberts, M. G. (2010). The construction of next-generation matrices for compartmental epidemic models. Journal of the royal society interface, 7(47), 873-885.

[31]. Van den Driessche, P., & Watmough, J. (2002). Reproduction numbers and sub-threshold endemic equilibria for compartmental models of disease transmission. Mathematical biosciences, 180(1-2), 29-48.

[32]. Bagkur, C., Guler, E., Kaymakamzade, B., Hincal, E., & Suer, K. (2022). Near future perspective of ESBL-Producing Klebsiella pneumoniae strains using mathematical modeling. CMES, 130, 111-32.

[33]. Abdullat, M., Hayajneh, W., Issa, A. B., Alshurman, A., Marar, B., Al-Hajajrah, A., ... & Wolfson, L. J. (2021). Use of health care resources for varicella in the paediatric population, Jordan. Eastern Mediterranean Health Journal, 27(2).

[34]. Sowole, S. O., Sangare, D., Ibrahim, A. A., & Paul, I. A. (2019). On the existence, uniqueness, stability of solution and numerical simulations of a mathematical model for measles disease. Int. J. Adv. Math, 4, 84-111.

[35]. Hethcote, H. W., & van den Driessche, P. (1991). Some epidemiological models with nonlinear incidence. Journal of Mathematical Biology, 29(3), 271-287.

[36]. Kaymakamzade, B., Baba, I. A., & Hincal, E. (2016). Global stability analysis of oseltamivir–resistant influenza virus model. Procedia Computer Science, 102, 333-341.

[37]. Islam, M. S., Asaduzzaman, M., & Mondal, M. N. I. (2014). Stability of an SVI Epidemic Model. IOSR Journal of Mathematics, 10(3), 51-58

[38]. Buonomo, B., & Vargas-De-León, C. (2012). Global stability for an HIV-1 infection model including an eclipse stage of infected cells. Journal of Mathematical Analysis and Applications, 385(2), 709-720.